Inorganic Chemistry
Article

Inorg. Chem. **2009**, *48*, 11821–11831 **11821**
DOI: 10.1021/ic901883h

Eight-Coordinate Zn(II), Cd(II), and Pb(II) Complexes Based on a 1,7-Diaza-12-crown-4 Platform Endowed with a Remarkable Selectivity over Ca(II)

Raquel Ferreirós-Martínez, David Esteban-Gómez,* Andrés de Blas, Carlos Platas-Iglesias, and Teresa Rodríguez-Blas*

Departamento de Química Fundamental, Universidade da Coruña, Campus da Zapateira, Alejandro de la Sota 1, 15008 A Coruña, Spain

Received September 23, 2009

The thermodynamic stability of the Pb(II), Cd(II), Zn(II), and Ca(II) complexes with the dianionic macrocyclic ligand *N,N′*-bis[(6-carboxy-2-pyridyl)methyl]-1,7-diaza-12-crown-4 (H_2bp12c4) has been investigated by pH-potentiometric titrations at 25 °C in 0.1 M KNO_3. The stability constants vary in the following order: Cd(II) > Zn(II) ∼ Pb(II) > Ca(II). As a consequence, H_2bp12c4 present an important Cd(II)/Ca(II) selectivity, as well as a certain selectivity for Cd(II) over Zn(II). To rationalize these results, a detailed investigation of the structure of these complexes has been carried out both in solid state and in aqueous solution. Furthermore, the [M(bp12c4)] complexes (M = Ca, Zn, Cd, or Pb) were characterized by means of density functional theory (DFT) calculations (B3LYP model) to obtain information on their solution structures and to investigate the possible stereochemical activity of the Pb(II) lone pair. Our results show that in all cases the metal ion is octacoordinated by the ligand, a situation that is particularly rare for Zn(II) complexes. The coordination polyhedra observed in the solid state for the [M(bp12c4)] complexes (M = Zn, Cd, or Ca) is closely related to the conformation adopted by the ligand in the corresponding complex: The Zn(II) complex adopts a $\Delta(\lambda\lambda\lambda\lambda)$ conformation in the solid state, which results in a square antiprismatic coordination, while the $\Delta(\delta\delta\delta\delta)$ conformation observed for the Cd(II) and Ca(II) analogues yields inverted-square antiprismatic geometries. The X-ray crystal structure of the Pb(II) analogue shows that the metal ion is directly bound to the eight donor atoms of the ligand, but the bond distances of the metal coordination environment indicate an asymmetrical coordination of the cation by the ligand, which is attributed to the stereochemical activity of the Pb(II) lone pair. In aqueous solution the Ca(II), Zn(II), and Cd(II) complexes show rigid C_2 symmetries, while the Pb(II) analogue presents a more flexible structure.

Introduction

The interest in the coordination chemistry of cadmium(II) and lead(II) in aqueous solution is related to the widespread industrial uses of their compounds and to their inherent toxicity and health effects.[1,2] Their presence in the aquatic environment has been of great concern because of their non biodegradable nature. Indeed, these metal ions are cumulative poisons, capable of being assimilated and stored in tissues of organisms, causing noticeable adverse physiological effects. Damage to the lung in cadmium exposed workers was the first human health effect related to cadmium in a report published already 70 years ago.[3] Exposure to Cd(II) causes bone diseases, gastrointestinal and renal dysfunction, and cadmium and cadmium compounds are regarded as carcinogenic to humans. Even when acute human intoxications with cadmium are rare, health effects due to chronic low-level cadmium exposure are still a problem in some industrial areas with high environmental cadmium pollution, creating a clinical need for chelation of aged cadmium deposits in the liver and kidney. Most lead poisoning results from ingestion or inhalation of *inorganic* lead [Pb(II)]. Lead poisoning particularly affects young children who can absorb up to 50% of ingested lead.[4] Once ingested through the gastrointestinal track, lead accumulates in soft tissues including vital organs as kidneys, liver, or brain, where it is bound to thiol and phosphate groups in proteins, nucleic acids, and cell membranes[5,6] originating severe neurological and/or hematological effects.[7]

*To whom correspondence should be addressed. E-mail: mayter@udc.es (T.R.-B.), desteban@udc.es (D.E.-G.).

(1) Harrison, R. M.; Laxen, D. R. H. *Lead Pollution*; Chapman and Hall: London, 1981.
(2) Nordberg, G. F. *BioMetals* **2004**, *17*, 485–489.
(3) Bulmer, F. M. R.; Rothwell, H. E.; Frankish, E. R. *Can. Pub. Health J.* **1938**, *29*, 19–26.
(4) Goyer, R. A. *Handbook on Toxicity of Inorganic Compounds*; Seiler, H. G., Sigel, A., Sigel, H., Eds.; Marcel Dekker: New York, 1988; pp 359−382.
(5) (a) Sigel, H.; Da Costa, C. P.; Martin, R. B. *Coord. Chem. Rev.* **2001**, *219−221*, 435–461. (b) Sigel, H.; Fischer, B. E.; Farkas, E. *Inorg. Chem.* **1983**, *22*, 925–934. (c) Tajimir-Riahi, H. A.; Langlais, M.; Savoie, R. *Nucleic Acids Res.* **1988**, *16*, 751–762. (d) Kazantis, G. *Poisoning, Diagnosis and Treatment*; Vale, J. A., Meredith, T. J., Eds.; Update Books: London, 1981; pp 171−175. (e) Baltrop, D. *Poisoning, Diagnosis and Treatment*; Vale, J. A., Meredith, T. J., Eds.; Update Books: London, 1981; pp 178−185.

Published on Web 11/13/2009

Because of the highly favored complexation arising from the chelate and macrocyclic effects, both chelate and macrocyclic ligands have been widely used for metal sequestering. Particularly interesting are the studies reported by Hancock concerning the factors that control the metal ion binding affinity, especially those related to the metal ion complementarity of ligand architectures.[8] In the case of macrocyclic ligands, three major strategies emerge for achieving effective complexation:[9,10] (**i**) the use of ring size variation to maximize the thermodynamic stability of the complex by matching the radius of the metal ion to the hole size of the macrocyclic ligand; (**ii**) the use of donor set variation to modify the affinities of the ligand systems toward particular metal ions; and (**iii**) the use of substituent variation to take advantage of the effect of appended substituents to the donor atoms of the parent macrocycle on metal ion discrimination.

The relative facility with which crown ethers can be functionalized with pendant arm(s) containing additional donor atom(s) enhances the cation binding ability and the selectivity of the parent crown ether.[11] Thus, lariat crown ethers often exhibit different cation binding properties from the parent crown ethers.[12] The two principal groups of lariat ethers are the C-pivot and the N-pivot lariat ethers. Of these two groups, the N-pivot molecules have proved to be quite flexible and strong cation binders while the C-pivot molecules have proved to be less flexible and to exhibit weaker cation binding strength.[13] A classical example of enhanced complex stability through the introduction of pendant arms on lariat ethers is the addition of hydroxyethyl arms to 4,13-diaza-18-crown-6, which results on a considerable increase in the formation constants of the corresponding lead(II) complexes in water (ca. 2.4 log K_1 units).[14] An example of metal ion discrimination by using a lariat ether based on a 4,13-diaza-18-crown-6 platform containing picolinate pendants has been recently reported by us.[15] This ligand shows an unprecedented selectivity for the large lanthanide(III) ions, with a dramatic drop of the stability observed from Ce(III) to Lu(III) as the radius of the lanthanide ion decreases (log K_{CeL} − log K_{LuL} = 6.9).

Scheme 1

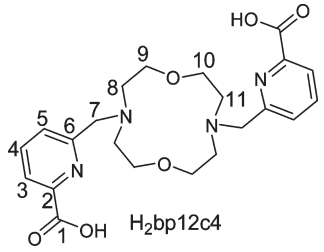

H_2bp12c4

In the search for new complexing agents with potential application in chelation treatment of Cd(II) and Pb(II) intoxication,[16] herein we report the complexation properties toward these metal ions of the macrocyclic ligand containing picolinate pendants H_2bp12c4 (Scheme 1). Moreover, we also investigated the complexation behavior of this ligand toward endogenously available metal ions such as Zn(II) and Ca(II). Thermodynamic stability constants of the Zn(II), Cd(II), Pb(II), and Ca(II) complexes of this ligand have been determined by pH potentiometric titrations. The structure of the complexes in solution has been studied by ^{1}H and ^{13}C NMR techniques in D_2O solution. The X-ray crystal structures of the [M(bp12c4)] (M = Zn, Cd, Pb, or Ca) and $[Zn(Hbp12c4)]^+$ complexes are also reported. To gain information about the solution structure of these complexes, as well as to understand the structural features and electronic properties related to the stereochemical activity of the lead(II) lone pair, the complexes have been also characterized by means of density functional theory (DFT) calculations (B3LYP model).

Experimental Section

General Methods. Elemental analyses were carried out on a Carlo Erba 1108 elemental analyzer. FAB mass spectra were recorded using a FISONS QUATRO mass spectrometer with a Cs ion-gun and 3-nitrobenzyl alcohol as matrix. IR-spectra were recorded using a Bruker Vector 22 spectrophotometer equipped with a Golden Gate Attenuated Total Reflectance (ATR) accessory (Specac). ^{1}H and ^{13}C NMR spectra were recorded at 25 °C on Bruker Avance 300 and Bruker Avance 500 spectrometers. For measurements in D_2O, *tert*-butyl alcohol was used as an internal standard with the methyl signal calibrated at δ = 1.2 (^{1}H) and 31.2 ppm (^{13}C). Spectral assignments were based in part on two-dimensional COSY, HMQC, and HMBC experiments.

Chemicals and Starting Materials. 6-Chloromethylpyridine-2-carboxylic acid methyl ester was prepared according to the literature method.[17] All other chemicals were purchased from commercial sources and used without further purification, unless otherwise stated.

Caution! *Although we have experienced no difficulties with the perchlorate salts, these should be regarded as potentially explosive and handled with care.*[18]

***N,N′*-Bis[(6-carboxy-2-pyridyl)methyl]-1,7-diaza-12-crown-4 (H_2bp12c4·2HCl·H_2O).** This compound was prepared by using

(6) (a) Da Costa, C. P.; Sigel, H. *Inorg. Chem.* **2000**, *39*, 5985–5993. (b) Martin, R. B. *Inorg. Chim. Acta* **1998**, *283*, 30–36. (c) Magyar, J. S.; Weng, T.-C.; Stern, Ch. M.; Dye, D. F.; Rous, B. W.; Payne, J. C.; Bridgewater, M. A.; Mijovilovich, B.; Parkin, G.; Zaleski, J. M.; Penner-Hahn, J. E.; Godwin, H. A. *J. Am. Chem. Soc.* **2005**, *127*, 9495–9505.

(7) (a) Lanphear, B. P.; Hornung, R.; Khoury, J.; Yolton, K.; Baghurst, P.; Bellinger, D. C.; Canfield, R. L.; Dietrich, K. N.; Bornschein, R.; Greene, T.; Rothenberg, S. J.; Needleman, H. L.; Schnaas, L.; Wasserman, G.; Graziano, J.; Roberts, R. *Environ. Health Perspect.* **2005**, *113*, 894–899. (b) Castellino, C.; Caselino, P.; Sannolo, N. *Inorganic Lead Exposure: Metabolism and Intoxication*; Lewis: Boca Raton, FL, 1994.

(8) (a) Hancock, R. D.; Martell, A. E. *Chem. Rev.* **1989**, *89*, 1875–1914. (b) Hancock, R. D.; Martell, A. E. *Supramolecular Chem.* **1996**, *6*, 401–407. (c) Hancock, R. D.; Maumela, H.; de Sousa, A. S. *Coord. Chem. Rev.* **1996**, *148*, 315–317. (d) Hay, B. P.; Hancock, R. D. *Coord. Chem. Rev.* **2001**, *212*, 61–78.

(9) Inoue, Y.; Gokel, G. W. *Cation Binding by Macrocycles. Complexation of Cationic Species by Crown Ethers*; Marcel Dekker: New York, 1990.

(10) (a) Izatt, R. M.; Pawlak, K.; Bradshaw, J. S.; Bruening, R. L. *Chem. Rev.* **1991**, *91*, 1721–1785. (b) Izatt, R. M.; Bradshaw, J. S.; Pawlak, K.; Bruening, R. L.; Tarbet, B. *J. Chem. Rev.* **1992**, *92*, 1261–1354. (c) Gokel, G. W. *Chem. Soc. Rev.* **1992**, *21*, 39–47. (d) Izatt, R. M.; Pawlak, K.; Bradshaw, J. S. *Chem. Rev.* **1995**, *95*, 2529–2586.

(11) (a) Gokel, G. W.; Korzeniowski, S. H. *Macrocyclic Polyether Synthesis*; Springer: Berlin, 1982; pp 6, 39.(b) Nakatsuji, Y.; Nakamura, T.; Yonetani, M.; Yuya, H.; Okahara, M. *J. Am. Chem. Soc.* **1988**, *110*, 531–538.

(12) Gokel, G. W. *Chem. Soc. Rev.* **1992**, *21*, 39–47, and references cited therein.

(13) Nakatsuji, Y.; Nakamura, T.; Okahara, M.; Dishong, D. M.; Gokel, G. W. *J. Org. Chem.* **1983**, *48*, 1237–1242.

(14) Damu, K. V.; Hancock, R. D.; Wade, P. W.; Boeyens, J. C. A.; Billing, D. G.; Dobson, S. M. *J. Chem. Soc., Dalton Trans.* **1991**, 293–298.

(15) Roca-Sabio, A.; Mato-Iglesias, M.; Esteban-Gomez, D.; Toth, E.; de Blas, A.; Platas-Iglesias, C.; Rodriguez-Blas, T. *J. Am. Chem. Soc.* **2009**, *131*, 3331–3341.

(16) (a) Andersen, O. *Chem. Rev.* **1999**, *99*, 2683–2710. (b) Blanusa, M.; Varnai, V. M.; Piasek, M.; Kostial, K. *Curr. Med. Chem.* **2005**, *12*, 2771–2794.

(17) Chrystal, E. J. T.; Couper, L.; Robins, D. J. *Tetrahedron* **1995**, *51*, 10241–10252.

(18) Wolsey, W. C. *J. Chem. Educ.* **1973**, *50*, A335–A337.

a slight modification of the literature method.[19] 6-Chloromethylpyridine-2-carboxylic acid methyl ester (2.50 g, 13.47 mmol) and Na_2CO_3 (7.30 g, 68.86 mmol) were added to a solution of 1,7-diaza-12-crown-4 (1.20 g, 6.89 mmol) in acetonitrile (60 mL). The mixture was heated to reflux with stirring for a period of 24 h, and then the excess of Na_2CO_3 was filtered off. The filtrate was concentrated to dryness, and the yellow residue partitioned between equal volumes (200 mL) of H_2O and CH_2Cl_2. The organic phase was separated, dried over $MgSO_4$, filtered, and evaporated to dryness to give a yellow solid. This was dissolved in 6 M HCl (10 mL), and the solution heated to reflux for 24 h. After cooling to room temperature the white solid formed was collected by filtration to give 2.55 g (69%) of the desired compound. Anal. Calcd for $C_{22}H_{28}N_4O_6 \cdot 2HCl \cdot H_2O$: C, 49.35; H, 6.02; N, 10.46%. Found: C, 48.88; H, 5.62; N, 10.87%. FAB-MS (*m*/*z*(%BPI)): 445(100) $[H_3bp12c4]^+$. δ_H (solvent D_2O, 298 K, 300 MHz, pD = 6.0): 8.00 (t, 2H, py); 7.98 (d, 2H, py); 7.67 (d, 2H, py); 4.56 (s, 4H, $-CH_2-$); 3.66 (t, 8H, $-CH_2-$); 3.49 (t, 8H, $-CH_2-$). δ_C (solvent D_2O, 298 K, 75.5 MHz, pD = 7.0): 66.6, 62.6, 56.1 (secondary C); 140.9, 129.1, 125.8 (tertiary C); 173.9, 155.2, 150.9 (quaternary C). IR: 1715 ν(C=O), 1599 $\nu(C{=}N)_{py}$ cm^{-1}.

[Pb(bp12c4)]·4Et$_3$NHClO$_4$ (1a). Triethylamine (0.212 mL, 1.521 mmol) was added to a suspension of $H_2bp12c4 \cdot 2HCl \cdot H_2O$ (0.204 g, 0.381 mmol) in 2-propanol (5 mL). The mixture was heated to reflux with stirring for a period of 0.5 h, and then a solution of $Pb(ClO_4)_2 \cdot 3H_2O$ (0.170 g, 0.419 mmol) in the same solvent (5 mL) was added. The resultant solution was heated to reflux for 2 h, filtered, and the filtrate concentrated to about 5 mL. Addition of diethylether resulted in the formation of a white solid, which was collected by filtration and dried under vacuum (yield 0.171 g, 36%). Anal. Calcd for $C_{22}H_{26}N_4O_6Pb \cdot 4Et_3NHClO_4$: C, 37.94; H, 6.23; N, 7.69%. Found: C, 37.80; H, 6.05; N, 7.75%. FAB-MS (*m*/*z*(%BPI)): 651(25) $[Pb(Hbp12c4)]^+$. IR: 1609 ν(C=O), 1570 $\nu(C{=}N)_{py}$ cm^{-1}. Slow evaporation of the mother-liquor gave single crystals of formula [Pb(bp12c4)]·2Et$_3$NHClO$_4$ (**1b**) suitable for X-ray diffraction analyses.

[Cd(bp12c4)]·2Et$_3$NHClO$_4$ (2). The preparation of this compound followed the same procedure as that described for **1** by using triethylamine (0.320 mL, 2.282 mmol), $H_2bp12c4 \cdot 2HCl \cdot H_2O$ (0.305 g, 0.570 mmol), and $Cd(ClO_4)_2$ (0.181 g, 0.581 mmol) in 10 mL of 2-propanol (yield 0.230 g, 63%). Anal. Calcd for $C_{22}H_{26}CdN_4O_6 \cdot 2Et_3NHClO_4$: C, 42.62; H, 6.10; N, 8.77%. Found: C, 41.99; H, 6.01; N, 8.69%. FAB-MS (*m*/*z*(%BPI)): 557(32) $[Cd(Hbp12c4)]^+$. IR: 1613 ν(C=O), 1582 $\nu(C{=}N)_{py}$ cm^{-1}. Slow evaporation of the mother-liquor gave single crystals of formula **2** suitable for X-ray diffraction analyses.

[Zn(bp12c4)]·2Et$_3$NHClO$_4$ (3a). The preparation of this compound followed the same procedure as that described for **1** by using triethylamine (0.224 mL, 1.521 mmol), $H_2bp12c4 \cdot 2HCl \cdot H_2O$ (0.215 g, 0.402 mmol), and $Zn(ClO_4)_2 \cdot 6H_2O$ (0.154 g, 0.414 mmol) in 10 mL of 2-propanol (yield 0.182 g, 50%). Anal. Calcd for $C_{22}H_{26}N_4O_6Zn \cdot 2Et_3NHClO_4$: C, 44.82; H, 6.42; N, 9.22%. Found: C, 43.07; H, 6.01; N, 9.08%. FAB-MS (*m*/*z*(%BPI)): 507(34) $[Zn(Hbp12c4)]^+$. IR: 1625 ν(C=O), 1591 $\nu(C{=}N)_{py}$ cm^{-1}. Slow evaporation of the mother-liquor gave single crystals of formula $[Zn_2(bp12c4)]Cl_2$ (**3b**) suitable for X-ray diffraction analyses. An analogous synthetic procedure in the absence of triethylamine gave single crystals of formula [Zn(Hbp12c4)]-$(ClO_4)_2 \cdot 2.5H_2O \cdot 0.5MeOH$ (**3c**) suitable for X-ray diffraction analyses.

[Ca(bp12c4)]·2Et$_3$NHClO$_4$ (4). The preparation of this compound followed the same procedure as that described for **1** by using triethylamine (0.288 mL, 2.066 mmol), $H_2bp12c4 \cdot 2HCl \cdot H_2O$ (0.277 g, 0.517 mmol), and $Ca(ClO_4)_2 \cdot 4H_2O$ (0.173 g, 0.556 mmol) in 10 mL of 2-propanol (yield 0.111 g, 24%). Anal. Calcd for $C_{22}H_{26}CaN_4O_6 \cdot 2Et_3NHClO_4$: C, 46.10; H, 6.60; N, 9.49%. Found: C, 45.15; H, 6.34; N, 9.31%. FAB-MS (*m*/*z*(%BPI)): 483(19) $[Ca(Hbp12c4)]^+$. IR: 1615 ν(C=O), 1582 $\nu(C{=}N)_{py}$ cm^{-1}. Slow evaporation of the mother-liquor gave single crystals of (**4**) suitable for X-ray diffraction analyses.

Potentiometry. Ligand protonation constants and stability constants with Zn(II), Cd(II), Pb(II), and Ca(II) were determined by pH-potentiometric titration at 25 °C in 0.1 M KNO_3. The samples (15 mL) were stirred while a constant Ar flow was bubbled through the solutions. The titrations were carried out adding a standardized KOH solution with a Metrohm Dosimat 794 automatic buret. KOH was standardized by potentiometric titration against potassium hydrogen phthalate. A glass electrode filled with 3 M KCl was used to measure pH. The stock solutions of MCl_2 (M = Ca, Zn, or Cd) and $Pb(NO_3)_2$ were prepared by dilution of the appropriate standards (Aldrich). The pH of the titration mixture was adjusted by addition of a known volume of standard HNO_3. The exact amount of acid present in the standard solutions was determined by pH measurement. $H_2bp12c4$ was checked for purity by NMR and elemental analysis before titration. The ligand and metal−ligand (1:1) solutions were titrated over the pH range $2.0 < pH < 11.0$. In the case of the metal−ligand (1:1) solutions reverse titrations were performed to check the reversibility of the system. Reverse titrations were carried out adding a standardized HNO_3 solution; the pH of the titration mixture was adjusted by addition of a known volume of standard KOH. The protonation and stability constants were calculated from simultaneous fits of three independent titrations with the program HYPERQUAD.[20] The errors given correspond to one standard deviation.

Computational Methods. All calculations were performed using hybrid DFT with the B3LYP exchange-correlation functional,[21,22] and the Gaussian 03 package (Revision C.01).[23] Full geometry optimizations of the [M(bp12c4)] (M = Ca, Zn, Cd, or Pb) systems were performed in vacuo by using the standard 6-31G(d) basis set for the ligand atoms and the LanL2DZ valence and effective core potential functions for the metals.[24] The stationary points found on the potential energy surfaces as a result of the geometry optimizations have been tested to represent energy minima rather than saddle points via frequency analysis. In aqueous solution relative free energies of the different conformations of the complexes were calculated from solvated single point energy calculations on the geometries optimized in vacuo. In these calculations solvent effects were evaluated by using the polarizable continuum model (PCM). In particular, we used the C-PCM variant[25] that employs

(19) Mato-Iglesias, M.; Roca-Sabio, A.; Palinkas, Z.; Esteban-Gomez, D.; Platas-Iglesias, C.; Toth, E.; de Blas, A.; Rodriguez-Blas, T. *Inorg. Chem.* **2008**, *47*, 7840–7851.

(20) Gans, P.; Sabatini, A.; Vacca, A. *Talanta* **1996**, *43*, 1739–1753.

(21) Becke, A. D. *J. Chem. Phys.* **1993**, *98*, 5648–5652.

(22) Lee, C.; Yang, W.; Parr, R. G. *Phys. Rev. B* **1988**, *37*, 785–789.

(23) Frisch, M. J.; Trucks, G. W.; Schlegel, H. B.; Scuseria, G. E.; Robb, M. A.; Cheeseman, J. R.; Montgomery, Jr., J. A.; Vreven, T.; Kudin, K. N.; Burant, J. C.; Millam, J. M.; Iyengar, S. S.; Tomasi, J.; Barone, V.; Mennucci, B.; Cossi, M.; Scalmani, G.; Rega, N.; Petersson, G. A.; Nakatsuji, H.; Hada, M.; Ehara, M.; Toyota, K.; Fukuda, R.; Hasegawa, J.; Ishida, M.; Nakajima, T.; Honda, Y.; Kitao, O.; Nakai, H.; Klene, M.; Li, X.; Knox, J. E.; Hratchian, H. P.; Cross, J. B.; Adamo, C.; Jaramillo, J.; Gomperts, R.; Stratmann, R. E.; Yazyev, O.; Austin, A. J.; Cammi, R.; Pomelli, C.; Ochterski, J. W.; Ayala, P. Y.; Morokuma, K.; Voth, G. A.; Salvador, P.; Dannenberg, J. J.; Zakrzewski, V. G.; Dapprich, S.; Daniels, A. D.; Strain, M. C.; Farkas, O.; Malick, D. K.; Rabuck, A. D.; Raghavachari, K.; Foresman, J. B.; Ortiz, J. V.; Cui, Q.; Baboul, A. G.; Clifford, S.; Cioslowski, J.; Stefanov, B. B.; Liu, G.; Liashenko, A.; Piskorz, P.; Komaromi, I.; Martin, R. L.; Fox, D. J.; Keith, T.; Al-Laham, M. A.; Peng, C. Y.; Nanayakkara, A.; Challacombe, M.; Gill, P. M. W.; Johnson, B.; Chen, W.; Wong, M. W.; Gonzalez, C.; Pople, J. A. *Gaussian 03*, Revision C.01; Gaussian, Inc.: Wallingford, CT, 2004.

(24) (a) Hay, P. J.; Wadt, W. R. *J. Chem. Phys.* **1985**, *82*, 270–283. (b) Hay, P. J.; Wadt, W. R. *J. Chem. Phys.* **1985**, *82*, 284–298. (c) Hay, P. J.; Wadt, W. R. *J. Chem. Phys.* **1985**, *82*, 299–310.

(25) Barone, V.; Cossi, M. *J. Phys. Chem. A* **1998**, *102*, 1995–2001.

Table 1. Crystal Data and Structure Refinement

	1b	2	3b	3c	4
formula	$C_{34}H_{58}Cl_2N_6O_{14}Pb$	$C_{34}H_{58}CdCl_2N_6O_{14}$	$C_{22}H_{28}Cl_2N_4O_7Zn_2$	$C_{45}H_{68}Cl_2N_8O_{26}Zn_2$	$C_{34}H_{58}CaCl_2N_6O_{14}$
MW	1052.95	958.16	662.12	1338.71	885.84
crystal system	orthorhombic	orthorhombic	monoclinic	monoclinic	orthorhombic
space group	$Pca2_1$	$Pbcn$	$C2/c$	$P2_1/c$	$Pbcn$
a/Å	12.3662(6)	22.6010(4)	31.181(2)	12.532(2)	22.423(4)
b/Å	22.599(1)	12.1990(2)	13.417(5)	28.823(4)	12.328(5)
c/Å	15.0562(8)	14.9570(3)	13.370(2)	15.644(2)	15.003(8)
α/deg	90	90	90	90	90
β/deg	90	90	113.276(9)	93.658(3)	90
γ/deg	90	90	90	90	90
V/Å^3	4207.7(4)	4123.8(1)	5138(2)	5639(1)	4147(3)
Z	4	4	8	4	4
T/K	100.0(2)	100.0(2)	100.0(2)	100.0(2)	100.0(2)
λ, Å (Mo Kα)	0.71073	0.71073	0.71073	0.71073	0.71073
D_{calc}/g cm^{-3}	1.662	1.543	1.712	1.577	1.419
μ/mm^{-1}	4.207	0.731	2.126	1.038	0.352
R_{int}	0.0682	0.0649	0.0915	0.0576	0.0571
reflns measd	8641	5138	5320	14009	3683
reflns obsd	6017	3515	3727	10044	2197
R_1[a]	0.0494	0.0633	0.0403	0.0455	0.0521
wR_2 (all data)[b]	0.1131	0.1921	0.0961	0.1158	0.1431

[a] $R_1 = \sum||F_o| - |F_c||/\sum|F_o|$. [b] $wR_2 = \{\sum w(F_o^2 - F_c^2)^2/\sum wF_o^4\}^{1/2}$.

conductor rather than dielectric boundary conditions. The solute cavity is built as an envelope of spheres centered on atoms or atomic groups with appropriate radii. Calculations were performed using an average area of 0.2 Å^2 for all the finite elements (tesserae) used to build the solute cavities. Free energies include both electrostatic and nonelectrostatic contributions and non-potential energy terms (that is, zero point energies and thermal terms) obtained from frequency analysis performed in vacuo. The wave functions of the [Pb(bp12c4)] complex were analyzed by natural bond orbital analyses, involving natural atomic orbital (NAO) populations and natural bond orbitals (NBO).[26,27]

X-ray crystal structure determinations. Three dimensional X-ray data were collected on a Bruker X8 APEXII CCD diffractometer. Data were corrected for Lorentz and polarization effects and for absorption by semiempirical methods[28] based on symmetry-equivalent reflections. Complex scattering factors were taken from the program SHELX97[29] running under the WinGX program system[30] as implemented on a Pentium computer. The structures were solved by direct methods with SHELXS-97[29] (**2**), Superflip[31] (**3b**), and SIR92[32] (**4**), or Patterson methods with DIRDIF99[33] (**1b** and **3c**), and all of them were refined[29] by full-matrix least-squares on F^2. For the five compounds all hydrogen atoms were included in calculated positions and refined in riding mode, except those of the water molecules that were located in a difference electron-density map and all the parameters fixed. Some least-squares restraints have to be imposed in every case (241 for **1b**, 239 for **2**, 15 for **3b**, 26 for **3c**, and 97 for **4**) to fix the positional disorder on perchlorate groups and/or solvent molecules. The crystal of the cadmium complex is heavily disordered with occupation factor of 0.41882 for the atoms labeled as A present in the neutral complex. The data obtained for **3b** have been cleaned up with SQEEZE[34] to avoid the problems generated by a disordered methanol molecule in a special position. Finally, refinement converged with anisotropic displacement parameters for all non-hydrogen atoms for all five crystals. Crystal data and details on data collection and refinement are summarized in Table 1.

Results and Discussion

Synthesis. Ligand H_2bp12c4 (Scheme 1) was obtained in four steps from dimethyl pyridine-2,6-dicarboxylate with an overall yield of 34% by using a slight modification of a previously reported procedure.[19] Compounds of formula [M(bp12c4)]·xEt$_3$NHClO$_4$ (M = Ca, Zn, Cd, x = 2; M = Pb, x = 4) can be easily prepared by reaction between H_2bp12c4·2HCl·H_2O and the corresponding metal perchlorate in the presence of 4 equiv of triethylamine. The IR spectra of the four complexes (KBr discs) show a band at about 1620 cm^{-1} corresponding to the asymmetric stretching mode of the coordinated carboxylate groups. Bands corresponding to the ν_{as}(Cl−O) stretching and δ_{as}(O−Cl−O) bending modes of the perchlorate groups appear at about 1090 and 623 cm^{-1}. In agreement with the proposed formula the absorption at 623 cm^{-1} clearly shows up without splitting, as befit uncoordinated anions.[35] The FAB-mass spectra display intense peaks due to [M(Hbp12c4)]$^+$ (M = Ca, Zn, Cd, or Pb), which confirms the formation of the complexes. The relative intensity of the signals of [M(bp12c4)] complexes and triethylammonium salts in the ^{1}H NMR spectra support the formula proposed on the basis of analytical data.

Ligand Protonation Constants and Stability Constants of the Metal Complexes. The protonation constants of bp12c4^{2-} as well as the stability constants of its metal

(26) Glendening, E. D.; Reed, A. E.; Carpenter, J. E.; Weinhold, F. *NBO*, version 3.1; **1998**.
(27) Reed, A. E.; Curtiss, L. A.; Weinhold, F. *Chem. Rev*. **1988**, *88*, 899–926.
(28) *SABADS*, Version 2004/1;Bruker AXS Inc.: Madison, WI, 2004.
(29) Sheldrick, G. M. *Acta Crystallogr*. **2008**, *A64*, 112–122.
(30) Farrugia, L. J. WinGX MS-Windows system of programs for solving, refining and analysing single crystal X-ray diffraction data for small molecules; *J. Appl. Crystallogr*. **1999**, *32*, 837−838.
(31) SUPERFLIP, Palatinus, L.; Chapuis, G. *J. Appl. Crystallogr*. **2007**, *40*, 786−790.
(32) SIR92, Altomare, A.; Cascarano, G.; Giacovazzo, C.; Guagliardi, A.; Burla, M. C.; Polidori, G.; Camalli, M. *J. Appl. Crystallogr*. **1994**, *27*, 435−435.
(33) *DIRDIF99*; Beurskens, P. T.; Beurskens, G.; de Gelder, R.; Garcia-Granda, S.; Gould, R. O.; Israel, R.; Smits, J. M. M. *The DIRDIF-99 program system, Technical Report of the Crystallography Laboratory*; University of Nijmegen: The Netherlands, 1999.
(34) *SQUEEZE*; Van der Sluis, P.; Spek, A. L. *Acta Crystallogr*. **1990**, *A46*, 194−201.
(35) Nakamoto, K. *Infrared and Raman Spectra of Inorganic and Coordination Compounds*, 5th ed.; J. Wiley: New York, 1997.

complexes formed with Ca(II), Zn(II), Cd(II), and Pb(II) were determined by potentiometric titration in 0.1 M KNO_3; the constants and standard deviations are given in Table 2. The ligand protonation constants are defined as in eq 1, and the stability constants of the metal chelates and the protonation constants of the complexes are expressed in eqs 2 and 3, respectively:

$$K_i = \frac{[H_iL]}{[H_{i-1}L][H^+]} \quad (1)$$

$$K_{ML} = \frac{[ML]}{[M][L]} \quad (2)$$

$$K_{MHL} = \frac{[MHL]}{[ML][H^+]} \quad (3)$$

Where L stands for $bp12c4^{2-}$.

The potentiometric curve of $bp12c4^{2-}$ (Figure 1) is indicative of two fairly strongly acidic sites and two weakly acidic sites. The data indicate that two protons are titrated below pH ~ 5.3, one between pH 5.3 and 7.7, and a fourth proton between 7.7 and 9.6. In comparison to edta,[36] $bp12c4^{2-}$ has a lower protonation constant for the first protonation step, while the second protonation constant is about 0.8 log K units lower in edta than in $bp12c4^{2-}$; these protonation processes occur on the amine nitrogen atoms. The higher protonation constant for the second protonation step of $bp12c4^{2-}$ in comparison to that of edta is attributed to a lower electrostatic repulsion between the two protonated amine nitrogen atoms in $bp12c4^{2-}$ as a consequence of the relatively long distance between them. This result is in line with the higher log K_2 value observed for dtpa when compared to edta; the second log K_i in dtpa corresponds to the protonation of one of the terminal nitrogen atoms, with displacement of the first proton from the central to the other terminal nitrogen atom.[37] The first and second protonation constants determined for $bp12c4^{2-}$ are somewhat lower for than for the bisacetate derivative of the same macrocycle ($ba12c4^{2-}$, Table 2).[38] This is in accordance with previous observations where a diminution of the amine basicity has been observed on replacement of acetate arms by 6-methyl-2-pyridinecarboxylate groups.[39] The last two protonation steps observed for $bp12c4^{2-}$ probably take place at the pyridylcarboxylate groups.[39]

Potentiometric titrations of $H_2bp12c4 \cdot 2HCl \cdot H_2O$ have been carried out in the presence of equimolar Ca(II), Zn(II), Cd(II), and Pb(II) ions to determine the stability constants of the metal complexes. The 1:1 titration curves with all metal ions (Figure 1) display an inflection at $a = 4$ (a = mol of OH^-/mol of ligand), as expected for the formation of [M(bp12c4)] species. Monoprotonated forms of the complexes have been detected over the pH range studied for the Ca(II), Zn(II), and Pb(II) complexes, while for the Cdbp12c4 system no evidence for the presence of protonated species has been obtained from the analysis of the potentiometric titration curves. The protonation of the complex probably occurs in one of the uncoordinated oxygen atoms of a picolinate group, as observed in the solid state structure of the $[Zn(Hbp12c4)]^+$ complex. The solid state structures of the [Zn(bp12c4)] and $[Zn(Hbp12c4)]^+$ complexes show that the protonation of one of the picolinate groups does not require partial decoordination of the ligand, the metal ion being eight-coordinated in both species (see below). The species distribution diagrams for the Zn(II) and Pb(II) complexes (Figure 2) show the presence of monoprotonated complex in solution at pH < 4.5, while the dissociation of the complexes occurs below pH ~ 4. In the case of the Ca(II) complex the protonation of the complex is observed already at pH < 6, while the dissociation of the complex

Table 2. Ligand Protonation Constants and Thermodynamic Stability Constants of $H_2bp12c4$ and Its Metal Complexes As Determined by pH-Potentiometry [I = 0.1 M KNO_3][a]

	$H_2bp12c4$	edta[b]	$H_2ba12c4$[c]
log K_1	8.67(1)	10.19	9.53
log K_2	6.90(1)	6.13	7.46
log K_3	3.42(1)	2.69	2.11
log K_4	1.67(1)	2.00	
log K_{CaL}	10.70(1)	10.6	8.50
log K_{CaHL}	3.76(3)		
log K_{ZnL}	15.48(1)	16.5	12.28
log K_{ZnHL}	2.31(4)		
log K_{CdL}	16.84(1)	16.5	14.09
log K_{PbL}	15.44(1)	18.0	12.43
log K_{PbHL}	2.52(8)		

[a] Data reported previously for edta and $H_2ba12c4$ are provided for comparison. [b] Ref 36. [c] Ref 38; $H_2ba12c4$ = *N*,*N*′-bis(carboxymethyl)-1,7-dioxa-4,7-diazacyclododecane.

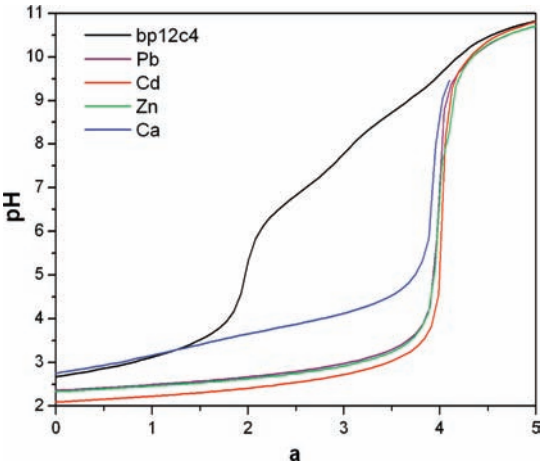

Figure 1. Experimental titration curves (pH vs a; a = mol of OH^-/mol ligand) for $H_2bp12c4 \cdot 2HCl \cdot H_2O$ in the presence and the absence of equimolar Pb(II), Cd(II), Zn(II), or Ca(II); $[L]_{tot} = 2 \cdot 10^{-3}$ M.

(36) (a) Lacoste, R. G.; Christoffers, G. V.; Martell, A. E. *J. Am. Chem. Soc.* **1965**, *87*, 2385–2388. (b) Martell, A. E.; Motekaitis, R. J.; Smith, R. M. *NIST Critically selected stability constants of metal complexes database*, Version 8.0 for windows; National Institute of Standards and Technology: Gaithersburg, MD, 2004; Standard Reference Data Program.

(37) Costa, J.; Tóth, É.; Helm, L.; Merbach, A. E. *Inorg. Chem.* **2005**, *44*, 4747–4755.

(38) Amorim, M. T. S.; Delgado, R.; Frausto da Silva, J. J. R. *Polyhedron* **1992**, *11*, 1891–1899.

(39) (a) Chatterton, N.; Gateau, C.; Mazzanti, M.; Pécaut, J.; Borel, A.; Helm, L.; Merbach, A. *Dalton Trans.* **2005**, 1129–1135. (b) Mato-Iglesias, M.; Balogh, E.; Platas-Iglesias, C.; Toth, E.; de Blas, A.; Rodriguez-Blas, T. *Dalton Trans.* **2006**, 5404–5415.

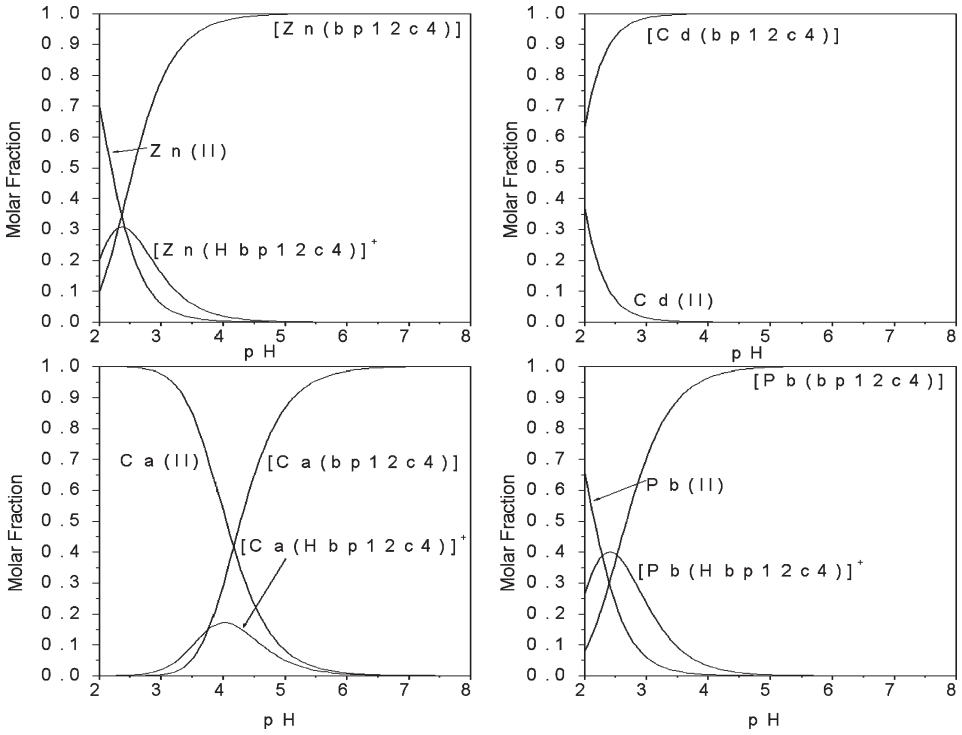

Figure 2. Species distribution of the M(bp12c4) systems (M = Ca, Zn, Cd or Pb), 1:1 M:L; [M(II)] = 1 mM, μ = 0.1 M (KNO_3), 25 °C.

occurs below pH ~ 6. Thus, the speciation diagrams shown in Figure 2 highlight the selectivity of H_2bp12c4 for Pb, Cd, and Zn over Ca. For instance Pb(II), Cd(II), and Zn(II) are almost totally complexed at pH 3.5 (98.5, 99.7, and 98.6%, respectively), while only 14.9% of the total Ca(II) is complexed under the same conditions.

The log K_{ML} values reported in Table 2 show that the stabilities of $bp12c4^{2-}$ complexes follow the trend Cd(II) > Zn(II) ~ Pb(II) > Ca(II). Thus, among the different metal ions studied $bp12c4^{2-}$ shows the highest affinity for Cd(II), a certain Cd/Zn and Cd/Pb selectivity being observed. The stabilities of $bp12c4^{2-}$ and $ba12c4^{2-}$ complexes follow the same trend, but the replacement of acetate pendants of $ba12c4^{2-}$ by picolinate groups increases significantly the complex stabilities. The Zn(II) and Pb(II) complexes of edta are more stable than the corresponding $bp12c4^{2-}$ analogues. In the case of Cd(II) the complex of $bp12c4^{2-}$ is slightly more stable than the edta one, a stability gain of 0.3 log units being observed.

Structural Study. The ^{1}H and ^{13}C NMR spectra of the [M(bp12c4)] complexes (M = Ca, Zn, Cd or Pb) were obtained in D_2O solution at about pD = 7.0. The proton spectra of the Ca(II), Zn(II), and Cd(II) complexes (Figure 3) consist of 13 signals corresponding to 13 magnetically non-equivalent proton environments in the ligand (see Scheme 1 for labeling), pointing to an effective C_2 symmetry of the complexes in solution. This is also confirmed by the ^{13}C NMR spectra, which show 11 peaks for the 22 carbon nuclei of the ligand backbone. The assignments of the proton signals (Table 3) were based on HMQC and HMBC 2D heteronuclear experiments as well as standard 2D homonuclear COSY experiments, which gave strong cross-peaks between the geminal CH_2 protons (7−11) and between the ortho-coupled pyridyl protons. Although the specific CH_2 proton assignments of the axial and equatorial H8−H11 protons were not possible on the basis of the 2D NMR spectra, they were carried out using the stereochemically dependent proton shift effects, resulting from the polarization of the C−H bonds by the electric field effect caused by the cation charge.[40] This results in a deshielding of the equatorial protons, which are pointing away from the metal ion. The signals due to protons H7a and H7b show an AB spin pattern where the larger shift for H7b results from the combined deshielding effects of the pyridyl ring current and the polarizing effect of the M(II) ion on the C−H bond pointing away from it.

The proton spectrum of the [Pb(bp12c4)] complex (Figure 3) consists of 8 signals, which points to an effective C_{2v} symmetry of the complex in solution. This is confirmed by the ^{13}C NMR spectrum, which shows 9 peaks for the 22 carbon nuclei of the ligand backbone. These results indicate that the Pb(II) complex presents a more flexible structure than the Ca(II), Zn(II), and Cd(II) analogues, which show a C_2 symmetry in solution. The signal due to the H7 protons is observed as a singlet, in contrast to the AB spectrum observed in the case of the Ca, Zn, and Cd analogues. However, H8ax and H8eq protons are observed as two separate signals at 2.83 and 3.00 ppm, respectively. These results indicate that the $\Delta \leftrightarrow \Lambda$ interconversion process is fast in the NMR time scale at room temperature, while the inversion of the five-membered chelate rings formed upon coordination of the crown moiety ($\delta \leftrightarrow \lambda$) is slow in the NMR time scale. The ^{1}H NMR spectrum recorded at 188 K in d_3-MeOD is virtually identical to that recorded in D_2O at room temperature, indicating a fast $\Delta \leftrightarrow \Lambda$ interconversion under these conditions.

(40) Harris, R. K. *Nuclear Magnetic Resonance Spectroscopy: A Physicochemical view*; Pitman: London, 1983.

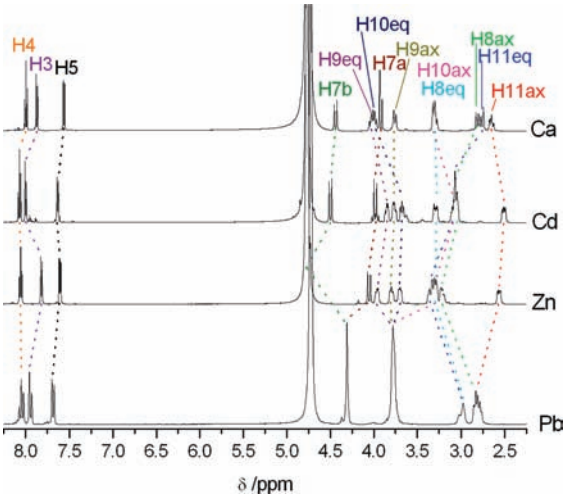

Figure 3. ^{1}H NMR spectra of [M(bp12c4)] complexes (M = Ca, Zn, Cd, or Pb) recorded in D_2O solution (pD = 7.0) at 298 K. See Scheme 1 for labeling.

Single crystals of formula $[M(bp12c4)]\cdot 2Et_3NHClO_4$ (M = Cd or Ca) have been obtained by slow evaporation of the mother liquor resulting from the reaction in 2-propanol of $H_2bp12c4\cdot 2HCl\cdot H_2O$ with the corresponding metal perchlorate in the presence of triethylamine. The analysis of the crystal structures indicates that both [M(bp12c4)] complexes (M = Ca or Cd) present a similar structure, which is not unexpected considering the similarity in the eight-coordinate effective ionic radii of Cd(II) (1.10 Å) and Ca(II) (1.12 Å).[41] These compounds crystallize in the orthorhombic space group *Pbcn*, and the asymmetric unit contains a half molecule. As a consequence, the [M(bp12c4)] complexes (M = Cd or Ca) show an undistorted C_2 symmetry in the solid state, where the symmetry axis is perpendicular to the pseudoplane described by the four donor atoms of the crown moiety and contains the metal ion. A view of the structure of the complexes is shown in Figure 4, while bond distances of the metal coordination environments are given in Table 4.

In both complexes the metal ion is directly bound to the eight donor atoms of the macrocyclic ligand, giving rise to eight-coordinate metal complexes. The distances between the metal ion and the oxygen atoms of the crown moiety are shorter than those between the metal ion and the pivotal nitrogen atoms, in contrast to the situation observed for the Zn(II) analogue (see below). The distances between the Cd(II) ion and the oxygen donor atoms of the picolinate pendants are close to those observed for the bis(dipicolinate) complex, while the distance between the Cd(II) ion and the nitrogen atoms of the pendant arms are intermediate between those observed in the bis- and tris-(dipicolinate) complexes.[42] The distances between the Cd(II) ion and the oxygen atoms of the crown moiety are about 0.07 Å longer than those observed in Cd(II) complexes of 12-crown-4,[43] but similar to those observed in complexes derived from 15-crown-5[44] or diaza-15-crown-5.[45] However, the $Cd-O_{crown}$ distances are clearly shorter than those observed in complexes derived from 18-crown-6[44] or diaza-18-crown-6.[46] In both complexes the side arms of the ligand are placed above the plane of the macrocyclic unit, resulting in a *syn* conformation. The *syn* conformation of the ligand in these complexes implies the occurrence of two helicities (one belonging to the crown moiety and one associated with the layout of the pendant arms).[47,48] Inspection of the crystal structure data reveals that two $\Delta(\delta\delta\delta\delta)$ and $\Lambda(\lambda\lambda\lambda\lambda)$ enantiomers co-crystallize in equal amounts (racemate).

Table 3. ^{1}H and ^{13}C NMR Shifts[a] of [M(bp12c4)] (M = Ca, Zn, Cd, or Pb) Complexes[b,c]

^{1}H	Ca[d]	Zn[e]	Cd[f]	Pb[g]	^{13}C	Ca	Zn	Cd	Pb
H3	7.87(d)	7.82(d)	8.03(d)	7.95(d)	C1	173.6	170.9	171.0	174.4
H4	8.00(t)	8.06(t)	8.07(t)	8.06(t)	C2	152.5	150.5	149.7	152.5
H5	7.56(d)	7.61(d)	7.63(d)	7.69(d)	C3	124.5	125.0	125.0	126.3
H7a	3.92(d)	4.05(d)	3.98(d)	4.32	C4	141.9	142.9	142.6	141.7
H7b	4.44(d)	4.74(d)	4.50(d)	4.32	C5	127.2	126.6	128.0	128.2
H8ax	2.84	3.23	3.07	2.83	C6	158.4	156.3	155.5	157.8
H8eq	3.30	3.29	3.29	3.00	C7	61.6	61.8	61.3	63.3
H9ax	3.77	3.80	3.76	3.79	C8	52.5	55.6	54.7	53.7
H9eq	4.04	3.97	3.85	3.79	C9	69.4	65.2	66.1	69.3
H10ax	3.31	3.31	3.06	3.79	C10	67.9	65.3	65.6	69.3
H10eq	4.00	3.71	3.68	3.79	C11	54.6	56.0	54.6	53.7
H11ax	2.66	2.57	2.51	2.83					
H11eq	2.76	3.35	3.10	3.00					

[a] Parts per million (ppm) with respect to TMS. [b] See Scheme 1 for labeling. [c] Assignment supported by 2D COSY, NOESY, HMQC and HMBC experiments at 298 K. [d] $^3J_{3,4}$ = 7.7 Hz; $^3J_{5,4}$ = 7.8 Hz; $^2J_{7a,7b}$ = $^2J_{7b,7a}$ = 15.8 Hz. [e] $^3J_{3,4}$ = 7.3 Hz; $^3J_{5,4}$ = 7.5 Hz; $^2J_{7a,7b}$ = $^2J_{7b,7a}$ = 16.6 Hz. [f] $^3J_{3,4}$ = 7.6 Hz; $^3J_{5,4}$ = 7.7 Hz; $^2J_{7a,7b}$ = $^2J_{7b,7a}$ = 15.7 Hz. [g] $^3J_{3,4}$ = 7.0 Hz; $^3J_{5,4}$ = 7.3 Hz; the spectra indicates an effective C_{2v} symmetry in solution (see text).

Zinc crystals of formula $[Zn_2(bp12c4)Cl_2]\cdot H_2O$ (**3b**) and $[Zn(Hbp12c4)](ClO_4)_2\cdot 2.5H_2O\cdot 0.5MeOH$ (**3c**) were also studied by X-ray diffraction. In **3b** one of the Zn(II) ions [Zn(1)] is endocyclically coordinated by the $bp12c4^{2-}$ ligand, while the second one [Zn(2)] is coordinated by two oxygen atoms of neighboring [Zn(bp12c4)] units and two chloride anions. This results in the formation of a one-dimensional (1D) coordination polymer (Figure 5). The Zn(1) ion is directly bound to the eight donor atoms of the macrocyclic ligand with bond distances ranging between 2.06 and 2.69 Å, which results in a rare eight-coordination around the metal ion. Indeed, only a few examples of eight-coordinate Zn(II) complexes have been reported to date. Eight-coordination has been observed in complexes containing the sandwich type complex cation $[Zn(12\text{-crown-}4)_2]^{2+}$.[49] However, to the best of our knowledge only one example of eight-coordinate Zn(II) complex has been reported to date in which the eight donor atoms are provided by a single polydentate ligand.[50] In

(41) Shannon, A. D. *Acta Crystallogr.* **1976**, *A32*, 751–767.
(42) (a) Aghabozorg, H.; Aghajani, Z.; Sharif, M. A. *Acta Crystallogr.* **2006**, *E62*, m1930–m1932. (b) Fu, A.-Y.; Wang, D.-Q.; Liu, A.-Z. *Acta Crystallogr.* **2004**, *E60*, m1372–m1373.
(43) (a) Zhang, H.; Wang, X.; Zhu, H.; Xiao, W.; Teo, B. K. *J. Am. Chem. Soc.* **1997**, *119*, 5463–5464. (b) Junk, P. C.; Smith, M. K.; Steed, J. W. *Polyhedron* **2001**, *20*, 2979–2988.
(44) Bond, A. H.; Rogers, R. D. *J. Chem. Crystallogr.* **1998**, *28*, 521–527.
(45) Esteban, D.; Bañobre, D.; de Blas, A.; Rodríguez-Blas, T.; Bastida, R.; Macías, A.; Rodríguez, A.; Fenton, D. E.; Adams, H.; Mahía, J. *Eur. J. Inorg. Chem.* **2000**, 1445–1456.
(46) Regueiro-Figueroa, M.; Esteban-Gomez, D.; Platas-Iglesias, C.; de Blas, A.; Rodríguez-Blas, T. *Eur. J. Inorg. Chem.* **2007**, 2198–2207.
(47) Corey, E. J.; Bailar, J. C., Jr. *J. Am. Chem. Soc.* **1959**, *81*, 2620–2629.
(48) Beattie, J. K. *Acc. Chem. Res.* **1971**, *4*, 253–259.
(49) Junk, P. C.; Smith, M. K.; Steed, J. W *Polyhedron* **2001**, *20*, 2979–2988.
(50) Beer, P. D.; Drew, M. G. B.; Leeson, P. B.; Ogden, M. I. *J. Chem. Soc., Dalton Trans.* **1995**, 1273–1283.

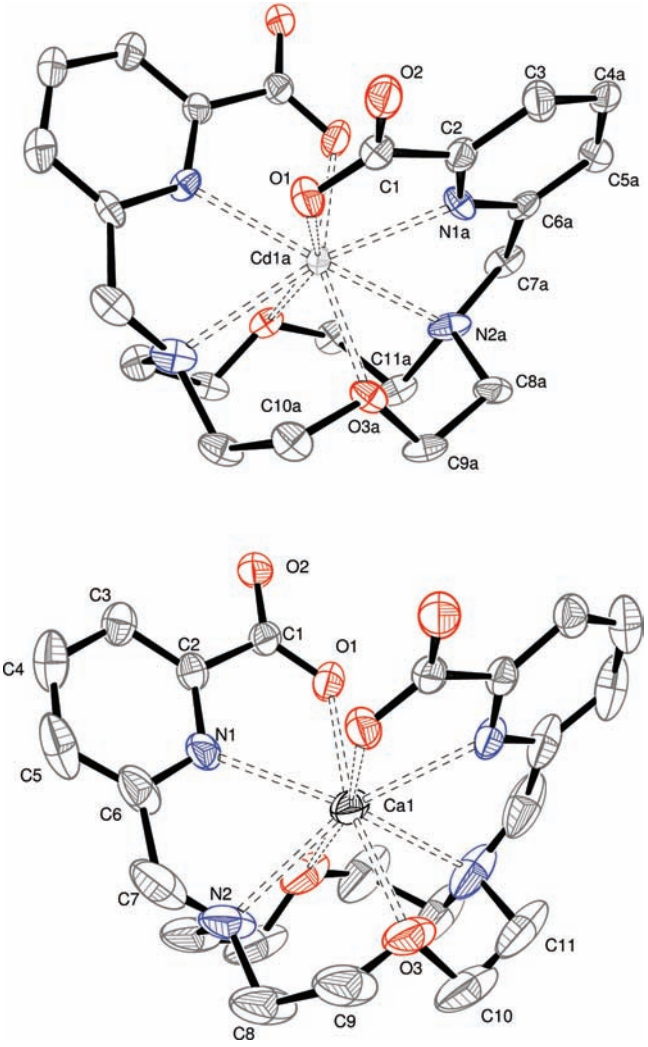

Figure 4. X-ray crystal structure of complexes [M(bp12c4)] (M = Cd, Ca) in **2** and **4** with atom labeling; hydrogen atoms are omitted for simplicity. The ORTEP plots are drawn at the 50% probability level.

[Zn(bp12c4)] the distances to the oxygen atoms of the crown moiety [Zn(1)−O(3) = 2.657(3) and Zn(1)−O(4) = 2.692(3) Å] are considerably longer than the remaining distances of the metal coordination environment (2.06−2.53 Å), indicating a relatively weak binding of these donors to the metal ion. The distances to the oxygen atoms of the crown moiety are similar to those observed for an octadentate Zn(II) complex of a functionalized calyx[4]arene,[50] but clearly longer than those reported for $[Zn(12\text{-crown-}4)_2]^{2+}$ (2.20−2.41 Å).[49] On the other hand, the Zn(2) ion is only four-coordinate in a slightly distorted tetrahedral environment, the bond angles of the metal coordination environment ranging from 106.1 to 112.6°. Both the Zn(2)−Cl and the Zn(2)−O bond distances are very close to those observed for other tetrahedral dichlorozinc(II) complexes.[51] The nitrogen atoms of the ligand provide the strongest bond to the Zn(1) ion, with Zn(1)−N bond distances ranging between 2.06 and 2.24 Å (Table 5). The distances between the Zn(1) and the oxygen atoms of the crown moiety [Zn(1)−O(3) = 2.657 Å, Zn(1)−O(4) = 2.692 Å] are longer than those between the metal ion and the oxygen atoms of the picolinate groups [Zn(1)−O(1) = 2.430 Å, Zn(1)−O(5) = 2.527 Å].

Table 4. Selected Bond Lengths (Å) for [Cd(bp12c4)] and [Ca(bp12c4)] Complexes in Compounds **2** and **4**[a]

[Cd(bp12c4)][b]		[Ca(bp12c4)][c]	
Cd(1A)−O(1)	2.375(8)	Ca(1)−O(1)	2.358(3)
Cd(1A)−N(1A)	2.40(1)	Ca(1)−N(1)	2.455(3)
Cd(1A)−O(3A)	2.41(1)	Ca(1)−O(3)	2.424(3)
Cd(1A)−N(2A)	2.73(1)	Ca(1)−N(2)	2.653(4)
Cd(1A)−O(1)#	2.375(8)	Ca(1)−O(1)#	2.358(3)
Cd(1A)−N(1A)#	2.40(1)	Ca(1)−N(1)#	2.455(3)
Cd(1A)−O(3A)#	2.41(1)	Ca(1)−O(3)#	2.424(3)
Cd(1A)−N(2A)#	2.73(1)	Ca(1)−N(2)#	2.653(4)

[a] See Figure 4 for labeling. [b] Symmetry transformations used to generate equivalent atoms: #1 $-x + 1$, y, $-z + 1/2$. [c] Symmetry transformations used to generate equivalent atoms: #1 $-x + 1$, y, $-z + 3/2$.

[Zn(Hbp12c4)](ClO$_4$)$_2$·2.5H$_2$O·0.5MeOH (**3c**) crystallizes in the monoclinic space group $P2_1/c$, and the asymmetric unit contains two different [Zn(Hbp12c4)](ClO$_4$)$_2$ complex salts with different bond distances and angles (Figure 6). The analysis of the crystal structure shows that in each of the molecules present in the asymmetric unit one of the oxygen atoms of a picolinate group [O(2) and O(8), Figure 6] is protonated. However, the Zn(II) ion maintains the eight-coordination observed for the unprotonated complex, the protonation of the ligand causing an important lengthening of the Zn(1)−O(1) and Zn(2)−O(7) bond distances (Table 2). The protonation of the complex also results in a substantial lengthening of the Zn−N(1) distance (ca. 0.07 Å), while the distances between the metal ion and the oxygen atoms of the crown moiety experience an important shortening (Table 5).

In both [Zn(bp12c4)] and $[Zn(Hbp12c4)]^+$ complexes the side arms of the ligand are placed above the plane of the macrocyclic unit, resulting in a *syn* conformation. Likewise, the lone pair of both pivotal nitrogen atoms is directed inward to the receptor cavity in an *endo-endo* arrangement. Inspection of the crystal structure data reveals that in both complexes two $\Delta(\lambda\lambda\lambda\lambda)$ and $\Lambda(\delta\delta\delta\delta)$ enantiomers co-crystallize in equal amounts (racemate).

The coordination polyhedron around the Zn(1) ion in [Zn(bp12c4)] can be described as a severely distorted square antiprism composed of two parallel pseudo planes: O(1), N(1), O(5), and N(4) define the upper pseudo plane (mean deviation from planarity 0.267 Å), while N(2), O(3), N(3), and O(4) define the lower pseudo plane (mean deviation from planarity 0.138 Å). The angle between these two least-squares planes amounts to 1.1°, and the Zn(1) ion is placed at 1.20 Å from the upper plane and 1.40 Å from the plane formed by N(2), O(3), N(3), and O(4). The mean twist angle, ω,[52] between these nearly parallel squares is 39.1°, a value that is close to that expected for a square antiprism (ideal value 45°). On the other hand, for the Cd(II) and Ca(II) analogues the coordination polyhedron around the metal ion can be

(51) (a) Priya, S. M. N.; Varghese, B.; Linet, J. M.; Das, S. J. *Acta Crystallogr.* **2007**, *E63*, m2318. (b) Liu, X.; Guo, G.-G.; Sun, Y.-Y. *Acta Crystallogr.* **2007**, *E63*, m275–m277. (c) Zhang, Z.-M.; Wang, D.-Q.; Xu, T.-T.; Gao, J. *Acta Crystallogr.* **2006**, *E62*, m3416–m3417. (d) Xu, X.-Y.; Xu, T.-T.; Ni, S.-S.; Gao, J.; Wang, D.-Q. *Acta Crystallogr.* **2006**, *E62*, m1548–m1549.

(52) Piguet, C.; Bünzli, J.-C. G.; Bernardinelli, G.; Bochet, C. G.; Froidevaux, P. *J. Chem. Soc., Dalton Trans.* **1995**, 83–97.

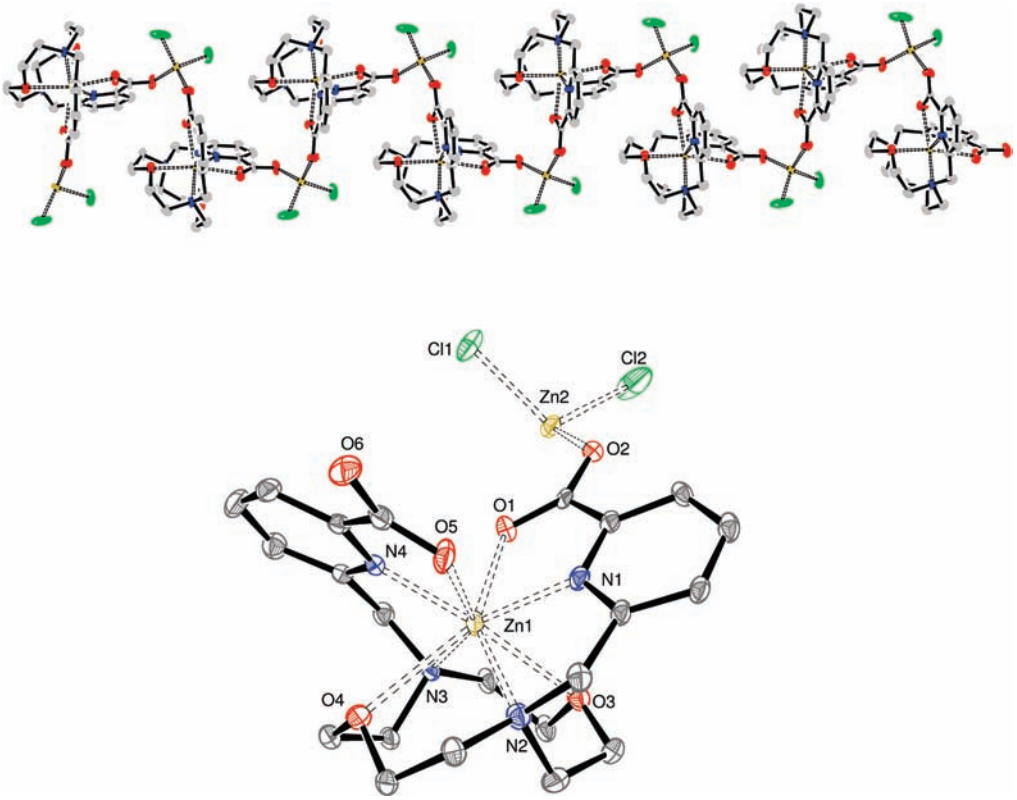

Figure 5. X-ray crystal structure of the $[Zn_2(bp12c4)Cl_2]_n$ complex in **3b** with atom labeling; hydrogen atoms are omitted for simplicity. The ORTEP plots are drawn at the 50% probability level.

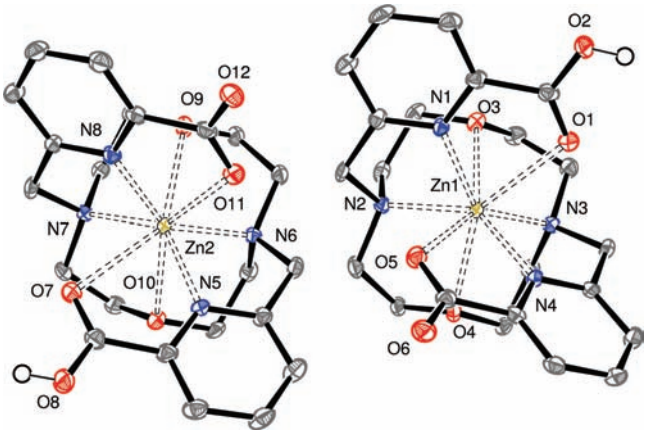

Figure 6. X-ray crystal structure of the cation $[Zn(Hbp12c4)]^+$ in **3c** with atom labeling; hydrogen atoms, except those protonating the picolinate moieties, are omitted for simplicity. The ORTEP plot is drawn at the 50% probability level.

described as an inverted-square antiprism composed of two parallel pseudo planes: N(1), N(1)#, O(1), and O(1)# define the upper pseudo plane (mean deviation from planarity (Å) 0.220 (Cd) and 0.329 (Ca)), while N(2), N(2)#, O(3), and O(3)# define the lower pseudo plane (mean deviation from planarity (Å) 0.143 (Cd) and 0.059 (Ca)). The mean twist angle, ω, between these parallel squares (0.0°) amounts to −27.5 (Cd) and −21.7° (Ca), which indicates an important distortion of the coordination polyhedra from a square antiprism (ideal value 45°) toward a regular prism (ideal value 0°). Thus, the coordination polyhedra observed for the [M(bp12c4)] complexes

Table 5. Selected Bond Lengths (Å) for $[Zn_2(bp12c4)Cl_2]$ and $[Zn(Hbp12c4)]^+$ Complexes in Compounds **3b** and **3c**[a]

$[Zn_2(bp12c4)Cl_2]$		$[Zn(Hbp12c4)]^+$	
Zn(1)−N(1)	2.061(3)	Zn(1)−N(1)	2.131(2)
Zn(1)−N(4)	2.074(3)	Zn(1)−N(4)	2.094(2)
Zn(1)−N(3)	2.230(3)	Zn(1)−N(3)	2.248(2)
Zn(1)−N(2)	2.238(3)	Zn(1)−N(2)	2.217(2)
Zn(1)−O(1)	2.430(3)	Zn(1)−O(1)	2.590(2)
Zn(1)−O(5)	2.527(3)	Zn(1)−O(5)	2.389(2)
Zn(1)−O(3)	2.657(3)	Zn(1)−O(3)	2.575(2)
Zn(1)−O(4)	2.692(3)	Zn(1)−O(4)	2.520(2)
Zn(2)−O(6)#1	1.962(3)	Zn(2)−N(8)	2.086(2)
Zn(2)−O(2)	1.971(3)	Zn(2)−N(5)	2.127(2)
Zn(2)−Cl(1)	2.259(1)	Zn(2)−N(6)	2.192(2)
Zn(2)−Cl(2)	2.2680(1)	Zn(2)−N(7)	2.237(2)
		Zn(2)−O(11)	2.444(2)
		Zn(2)−O(9)	2.539(2)
		Zn(2)−O(10)	2.634(2)
		Zn(2)−O(7)	2.686(2)

[a] See Figures 5 and 6 for labeling.

(M = Zn, Cd, or Ca) appears to be closely related to the conformation adopted by the ligand in the corresponding complex. Thus, the $\Delta(\lambda\lambda\lambda\lambda)$ conformation observed for the Zn(II) complex appears to favor a square antiprismatic coordination, while the $\Delta(\delta\delta\delta\delta)$ conformation observed for the Cd(II) and Ca(II) analogues yields inverted-square antiprismatic geometries. The situation is analogous to that observed for the lanthanide DOTA complexes.[53] Indeed, the $[Ln(DOTA)]^-$ complexes exist in solution as

(53) (a) Aime, S.; Botta, M.; Ermondi, G. *Inorg. Chem.* **1992**, *31*, 4291–4299. (b) Aime, S.; Botta, M.; Fasano, M.; Marques, M. P. M.; Geraldes, C. F. G. C.; Pubanz, D.; Merbach, A. E. *Inorg. Chem.* **1997**, *36*, 2059–2068.

two enantiomeric pairs of diasteroisomers; the $\Delta(\lambda\lambda\lambda\lambda)$ [or $\Lambda(\delta\delta\delta\delta)$] isomers show ω angles of about 40° with a square antiprismatic geometry, while the $\Delta(\delta\delta\delta\delta)$ [or $\Lambda(\lambda\lambda\lambda\lambda)$] ones have ω angles of about −30° and a inverted-square antiprismatic coordination. An inverted-antiprismatic coordination environment has been also found for $[Ca(DOTA)]^{2-}$ in the solid state.[54]

Figure 7 shows a view of the [Pb(bp12c4)] complex, while bond lengths of the metal coordination environment are listed in Table 6. The metal ion is directly bound to the eight donor atoms of the ligand. However, the bond distances of the metal coordination environment indicate an asymmetrical coordination of the metal ion by the ligand, with the Pb(1A)−O(5) and Pb(1A)−O(4) bond distances being substantially shorter than the Pb(1A)−O(1) and Pb(1A)−O(3) ones (Table 6). The conformation adopted by the $bp12c4^{2-}$ ligand in [Pb(bp12c4)] is clearly different than that observed for the Zn(II), Cd(II), and Ca(II) analogues. The later complexes show a slightly distorted (Zn) or undistorted (Cd and Ca) C_2 symmetry in the solid state, where the symmetry axis is perpendicular to the pseudoplane described by the four donor atoms of the crown moiety and contains the metal ion. In the case of the Pb(II) complex the plane described by the picolinate unit containing N(1) is nearly perpendicular to the best plane described by the four donor atoms of the crown moiety (77.4°), while the picolinate pendant containing N(4) is tilted toward O(4). This disposition of the pendant arms of the ligand results in the formation of an identifiable void in the liganding around the metal ion that is not observed in the case of the Zn(II), Cd(II), and Ca(II) analogues (Figure 7). This is typical of the so-called hemidirected compounds, in which the lone pair of electrons can cause a nonspherical charge distribution around the Pb(II) cation.[55,56] The void in the ligandind is accompanied by a concomitant shortening of the Pb(1A)−O(5) bond [2.434(10) Å], which is on the side of the Pb(II) ion away from the site of the stereochemically active lone pair, when compared to the Pb(1A)−O(1) one [2.569(8) Å]. Thus, the different structure observed for the Pb(II) complex of $bp12c4^{2-}$ in the solid state when compared to that of the Zn(II) and Cd(II) analogues appears to be related to the stereochemical activity of the Pb(II) lone pair. The stereochemical activity of the Pb(II) lone pair also results in a mixed conformation of the four chelate rings formed by the coordination of the $N-CH_2-CH_2-O$ units. Indeed, inspection of the crystal structure data reveals that two $\Delta(\delta\delta\delta\lambda)$ and $\Lambda(\lambda\lambda\lambda\delta)$ enantiomers co-crystallize in equal amounts.

To obtain information on the solution structure of the [M(bp12c4)] complexes (M = Ca, Zn, Cd, or Pb), as well as to investigate the possible stereochemical activity of the Pb(II) lone pair, these systems were characterized by means of DFT calculations (B3LYP model). On the grounds of our previous experience,[46,56a,57] in these calculations the 6-31G(d) basis set was used for the ligand atoms, while for the metals the effective core potential of Wadt and Hay (Los Alamos ECP) included in the LanL2DZ basis set was applied. Compared to all-electron basis sets, ECPs account for relativistic effects to some extent. It is believed that relativistic effects will become important for the elements from the fourth row of the periodic table.

The ^1H and ^{13}C NMR spectra of the Zn(II), Cd(II), and Ca(II) complexes of bp12c4 show a rigid C_2 symmetry in solution. There are eight possible conformations of the complexes of bp12c4 (four enatiomeric pairs of diasteroisomers) consistent with a C_2 symmetry.[19] Since enantiomers have the same physicochemical properties in a nonchiral environment we have considered the following four diasteroisomeric forms of the [M(bp12c4)] complexes (M = Ca, Zn, or Cd) in our conformational analysis: $\Delta(\lambda\lambda\lambda\lambda)$, $\Delta(\delta\delta\delta\delta)$, $\Delta(\delta\lambda\delta\lambda)$, and $\Delta(\lambda\delta\lambda\delta)$. The relative free energies of the $\Delta(\lambda\lambda\lambda\lambda)$, $\Delta(\delta\lambda\delta\lambda)$, and $\Delta(\lambda\delta\lambda\delta)$ conformations with respect to the $\Delta(\delta\delta\delta\delta)$ one were calculated in aqueous solution from solvated single point energy calculations (C-PCM model) on the geometries optimized in vacuo. The optimized Cartesian coordinates for the four diasteroisomeric forms of each complex are given as Supporting Information. The main results of these calculations are reported in Table 7 and Figure 8. Relative free energies were calculated as $\Delta G^{sol} = G^{sol}_X - G^{sol}_{\Delta(\delta\delta\delta\delta)}$, and therefore a positive

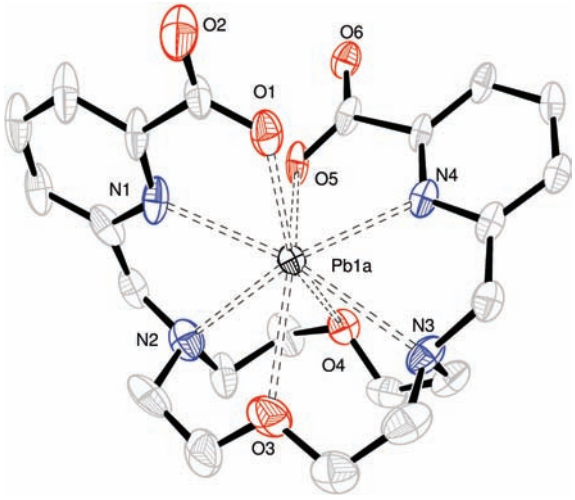

Figure 7. X-ray crystal structure of complex [Pb(bp12c4)] in **1b** with atom labeling; hydrogen atoms are omitted for simplicity. The ORTEP plot is drawn at the 50% probability level.

Table 6. Selected Bond Lengths (Å) for [Pb(bp12c4)] in Compound **1**[a]

Pb(1A)−O(5)	2.43(1)	Pb(1A)−O(4)	2.655(7)
Pb(1A)−N(4)	2.549(8)	Pb(1A)−O(3)	2.718(8)
Pb(1A)−O(1)	2.569(8)	Pb(1A)−N(2)	2.78(1)
Pb(1A)−N(1)	2.575(11)	Pb(1A)−N(3)	2.812(8)

[a] See Figure 7 for labeling.

(54) Anderson, O. P.; Reibenspies, J. H. *Acta Crystallogr.* **1996**, *C52*, 792–795.
(55) Shimoni-Livny, L.; Glusker, J. P.; Bock, C. W. *Inorg. Chem.* **1998**, *37*, 1853.
(56) (a) Esteban-Gómez, D.; Platas-Iglesias, C.; Enríquez-Pérez, T.; Avecilla, F.; de Blas, A.; Rodríguez-Blas, T. *Inorg. Chem.* **2006**, *45*, 5407–5416. (b) Pellissier, A.; Bretonniere, Y.; Chatterton, N.; Pecaut, J.; Delangle, P.; Mazzanti, M. *Inorg. Chem.* **2007**, *46*, 3714–3725.
(57) (a) Ferreiros-Martinez, R.; Esteban-Gomez, D.; Platas-Iglesias, C.; de Blas, A.; Rodriguez-Blas, T. *Dalton Trans.* **2008**, 5754–5765. (b) Platas-Iglesias, C.; Esteban-Gomez, D.; Enriquez-Perez, T.; Avecilla, F.; de Blas, A.; Rodriguez-Blas, A. *Inorg. Chem.* **2005**, *44*, 2224–2233. (c) Esteban-Gomez, C.; Platas-Iglesias, C.; Avecilla, F.; de Blas, A.; Rodriguez-Blas, T. *Eur. J. Inorg. Chem.* **2007**, 1635–1643.

Table 7. Relative Free Energies in Aqueous Solution (C-PCM, B3LYP/6-31G(d)) of Different Conformations of [M(bp12c4)] (M = Zn, Cd, Pb, or Ca) and $[M(Hbp12c4)]^+$ Complexes (M = Zn) with Respect to the $\Delta(\delta\delta\delta\delta)$ One[a]

	$\Delta(\lambda\lambda\lambda\lambda)$	$\Delta(\delta\lambda\delta\lambda)$	$\Delta(\lambda\delta\lambda\delta)$	$\Delta(\delta\delta\delta\lambda)$
[Ca(bp12c4)]	0.77	0.60	7.46	b
[Pb(bp12c4)]	1.85	4.05	6.76	−0.35
[Cd(bp12c4)]	1.60	1.44	8.03	b
[Zn(bp12c4)]	1.19	3.38	7.67	b
$[Zn(Hbp12c4)]^+$	0.18	2.93	9.03	b

[a] $\Delta G^{sol} = G^{sol}_X - G^{sol}_{\Delta(\delta\delta\delta\delta)}$, and therefore a positive relative energy indicates that the $\Delta(\delta\delta\delta\delta)$ conformation is more stable than the X one. Values in kcal mol^{-1}. [b] Not calculated.

relative energy indicates that the $\Delta(\delta\delta\delta\delta)$ conformation is more stable than the X one. According to our DFT calculations the $\Delta(\delta\delta\delta\delta)$ conformation is the most stable one for the Cd(II) and Ca(II) complexes, the relative order of stability being $\Delta(\delta\delta\delta\delta) > \Delta(\delta\lambda\delta\lambda) \sim \Delta(\lambda\lambda\lambda\lambda) > \Delta(\lambda\delta\lambda\delta)$. Thus, in the case of the Ca(II) and Cd(II) complexes the conformation observed in the solid state is that predicted to be the minimum energy conformation in aqueous solution by our DFT calculations, and these complexes most likely adopt the same conformation in the solid state and in aqueous solution.

In the case of the Zn(II) complex our calculations indicate that the $\Delta(\delta\delta\delta\delta)$ conformation is the most stable one, while a $\Delta(\lambda\lambda\lambda\lambda)$ conformation has been observed in the solid state. However, it must be pointed out that the two solid state structures obtained for the Zn(II) complex of $bp12c4^{2-}$ (see above) correspond either to the protonated form of the complex or to a 1D coordination polymer containing Zn(II) ions both endo- and exomacrocyclicly coordinated. To evaluate the effect of ligand protonation in the relative stabilities of the Zn(II) complex of $bp12c4^{2-}$ we have also performed geometry optimizations on the $[Zn(Hbp12c4)]^+$ system. The relative free energies obtained in solution for this system (Table 7) show that the protonation of the ligand provokes an important stabilization of the $\Delta(\lambda\lambda\lambda\lambda)$ conformation with respect to the $\Delta(\delta\delta\delta\delta)$ one. The protonation of the complex reduces the free energy difference between the $\Delta(\delta\delta\delta\delta)$ and $\Delta(\lambda\lambda\lambda\lambda)$ conformation to only 0.18 kcal·mol^{-1}. Thus, in its neutral form the Zn(II) complex most likely adopts a $\Delta(\delta\delta\delta\delta)$ conformation in aqueous solution.

For the Pb(II) complex our DFT calculations indicate that the conformation observed in the solid state, $\Delta(\delta\delta\delta\lambda)$ is also the most stable one in aqueous solution (Figure 8). This is probably linked to the stereochemical activity of the Pb(II) lone pair, which favors an asymmetric coordination of the Pb(II) ion by the ligand. An analysis of the natural bond orbitals (NBOs) shows that the Pb(II) lone pair orbital possesses a predominant 6s character, but it is polarized by a substantial 6p contribution: s[96.67%] p[3.33%]. Similar p contributions (1.89−4.39%) have been calculated for different hemidirected four-coordinate Pb(II) complexes with neutral ligands, while p contributions in the range 2.62−15.72% have been calculated for hemidirected four-coordinate Pb(II) complexes with anionic ligands.[55] These results clearly confirm that the Pb(II) lone pair is stereochemically active in the [Pb(bp12c4)] complex.

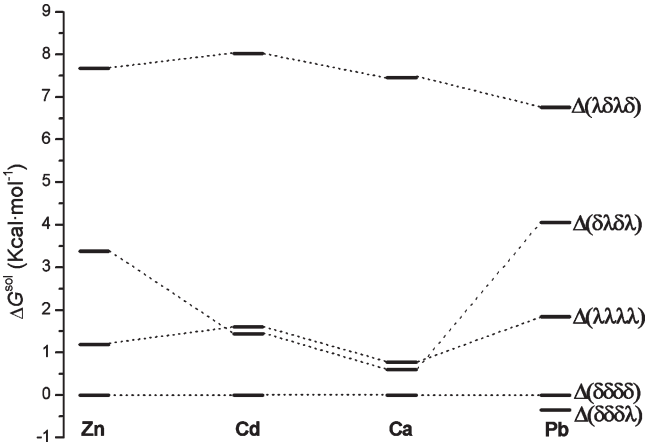

Figure 8. In aqueous solution C-PCM relative free energies of the different diasterisomeric forms of [M(bp12c4)] complexes (M = Zn, Cd, Ca, or Pb).

Conclusions

The octaadentate ligand $H_2bp12c4$ forms thermodynamically stable Ca(II), Zn(II), Cd(II), and Pb(II) complexes in aqueous solution. The stability constants vary in the following order: Cd(II) > Zn(II) ∼ Pb(II) > Ca(II). As a consequence, the complexes of $bp12c4^{2-}$ present an important Cd(II)/Ca(II) selectivity, as well as a certain selectivity for Cd(II) over Zn(II). A detailed investigation of the structure of these complexes shows that in all cases the metal ion is octacoordinated by the ligand. The Ca(II), Zn(II), and Cd(II) complexes show rigid C_2 symmetries in aqueous solution, while the Pb(II) analogue presents a more flexible structure. This appears to be related to the stereochemical activity of the Pb(II) lone pair that results in an asymmetrical coordination of this metal ion by the ligand. We are currently investigating chemical modifications of the ligand that could result in enhanced selectivities for Cd(II) and/or Pb(II) over endogeneous metal ions such as Ca(II) or Zn(II), thereby providing systems with potential application for the elimination of these metal ions from living bodies.

Acknowledgment. The authors thank Xunta de Galicia (PGIDIT06TAM10301PR and INCITE08ENA103005ES) for generous financial support. The authors are indebted to Centro de Supercomputación de Galicia (CESGA) for providing the computer facilities.

Supporting Information Available: In vacuo optimized Cartesian coordinates (Å) for the [M(bp12c4)] (M = Zn, Cd, Pb, or Ca) and $[Zn(Hbp12c4)]^+$ complexes and X-ray crystallographic data in CIF format. This material is available free of charge via the Internet at http://pubs.acs.org.